Large-scale synthesis and characterisation of Ag/Bi_2Te_3 superlattice nanowires via pulse electrodeposition

Junli Fu[1], Jinan Shi[2], Min Zhu[1], Yujie Liang[1], Guling Zhang[1], Honglong Shi[1], Hua Li[3], Bin Zou[1], Zhen Qu[1], Ying Jia[1], Wenzhong Wang[1]

[1]*School of Science, Minzu University of China, Beijing 100081, People's Republic of China*
[2]*Institute of Physics Chinese Academy of Sciences, Beijing 100190, People's Republic of China*
[3]*School of Life and Environmental Science, Minzu University of China, Beijing 100081, People's Republic of China*
E-mail: fujl08@muc.edu.cn

Published in Micro & Nano Letters; Received on 2nd November 2012; Revised on 1st February 2013; Accepted on 6th February 2013

Ag/Bi_2Te_3 superlattice nanowire arrays have been fabricated by pulse electrodeposition using porous anodic aluminium oxide as the template at large-scale quantity. The nanowire arrays were characterised by X-ray diffraction, a scanning electron microscope, a transmission electron microscope and high-resolution transmission electron microscopy (HRTEM). The results indicate that the nanowires are composed of the Bi_2Te_3 rhombohedral lattice phase and the Ag cubic lattice phase with alternately ordered multi-segment characters. The feature of dark segments alternated with bright segments can be easily distinguished because of the obvious heterogeneous contrast. The length of each segment varies from 25 to 45 nm. The HRTEM result shows that the composition of one segment is Ag and the neighbouring segment is Bi_2Te_3.

1. Introduction: Thermoelectric materials are attracting renewed interest because of increasing demands in energy and decreasing fuel supplies [1]. Good targets for thermoelectric materials are Bi_2Te_3 and its derived alloys at room temperature. A figure of merit of ~3 for these materials is necessary to compete with conventional compressor-based refrigerators and power sources [2].

It is found that low-dimensional, or quantum-confined, systems will have greater efficiencies compared with bulk materials [3]. In recent years, many one-dimensional (1D) thermoelectric materials, such as $Bi_{2-x}Sb_xTe_3$, $Bi_2Te_{3-y}Se_y$ and Bi_2Te_3 nanowires and nanotubes, have been synthesised by various methods [4–6]. Until now, the highest figure of merit, ZT of ~2.4 in the Bi_2Te_3/Sb_2Te_3 superlattice film was reported by Venkatasubramanian *et al.* [7]. Moreover, theoretical calculations predict that further enhancement of the thermoelectric figure of merit can be achieved in superlattice nanowires (SLNWs). In addition, it has been reported that the thermoelectric materials doped with metal particles can enhance their figure of merit. For instance, recent work showed that different Ag concentrations doped in Bi–Sb–Te alloys reveal a reduction of thermal conductivities and significant enhancement of electrical conductivities, leading to the improvement of figure of merit ZT [8, 9]. Considering the novel thermoelectric property and important applications, preparation of Bi_2Te_3/Ag SLNWs is valuable.

To fabricate the SLNWs, several kinds of strategies have been successfully developed in recent years. For example, Wang and co-workers [10] synthesised $InGaO_3/ZnO$ SLNWs via a catalyst assisted vapour–liquid–solid growth mechanism. Yang and co-workers [11] developed a hybrid pulsed laser ablation/chemical vapour deposition method for synthesising the high-quality Si/SiGe SLNWs. Wang *et al.* [12] fabricated the Bi_2Te_3/Te SLNWs using the precipitation reaction of the supersaturated $Bi_{0.26}Te_{0.74}$ alloy under a nanoconfined system. Among these various fabricating methods, the template-based electrochemical deposition method is widely used to prepare SLNWs. The advantage of this method is that it is able to tailor the composition and length of individual segments of nanowires by alternating the deposition potential and deposition time [13]. A variety of thermoelectric SLNWs, such as Bi/Sb [14], Bi_2Te_3/Sb [15], Bi/BiSb [16] and BiTe/BiSbTe [17], have been fabricated using a template-based electrochemical method. In this study, we electrodeposited Ag/Bi_2Te_3 SLNWs by porous anodic alumina oxide (AAO) template-assisted pulsed electrodeposition technology, and studied the morphology and phase structure of the as-prepared Ag/Bi_2Te_3 SLNWs.

2. Experiment section: The AAO templates used in our experiment were fabricated in 0.3 M oxalic acid solution at 40 V_{DC} by a two-step anodising process. Electrodeposition of Ag/Bi_2Te_3 SLNWs was performed in a three-electrode electrochemical cell on a CHI 760C electrochemical workstation. In the cell, a platinum plate, saturated calomel electrode (SCE), and the AAO template were used as counter, reference and working electrodes, respectively. The electrolyte solution consisted of $AgNO_3$ (0.01 M), $Bi(NO_3)_3{\cdot}5H_2O$ (0.075 M), $HTeO_2^+$ (0.1 M) in 1 M HNO_3. The deposition potential was alternately pulsed between a constant potential of −0.3 V (against SCE) to deposit a majority of Ag segment and a potential of −1.3 V (against SCE) to obtain the Bi_2Te_3 segment.

The morphology, size and microstructures of the nanowire arrays were obtained by a transmission electron microscope (TEM, JEM 2010) and a scanning electron microscope (SEM, HitachiS-4800). The phase structure of the as-prepared products was investigated by means of X-ray diffraction (XRD), using a general XD-3 diffractometer, with Cu K_α radiation ($\lambda = 1.54056$ Å).

3. Results and discussion: The cyclic voltammograms of Ag–Bi–Te electrolyte solution as well as the separated Bi–Te solution and Ag solution are shown in Fig. 1*a*. The cyclic voltammogram result of Ag–Bi–Te electrolyte solution clearly shows that the reduction range of Bi–Te and Ag extends from −0.2 V in the cathodic scanning process with a scanning rate of 100 mV/s. From the cyclic voltammogram results of separated Bi–Te solution and Ag solution, it can be seen that the reduction of Bi^{3+} and $HTeO^{2+}$ to BiTe begins at −0.4 V, whereas the reduction potential range of Ag^+ to Ag is from −0.1 V. From the above studies, two deposition potentials (i.e. −0.3 and −1.3 V) were selected to deposit Ag/Bi_2Te_3 SLNWs with pulse electrodeposition. An average potential V_{Ag} of −0.3 V was applied for t_{Ag} of 50 s to prepare the Ag segment, followed with an average potential V_{Bi2Te3} of −1.3 V for t_{Bi2Te3} of 150 s to prepare the majority of Bi_2Te_3 segments. The majority of Bi_2Te_3 segments can be deposited because the concentration of Bi^{3+} and $HTeO_2^+$ was higher than that of Ag^+. Typical applied-potential waveforms and their corresponding currents are shown in Fig. 1*b*.

doi: 10.1049/mnl.2012.0850

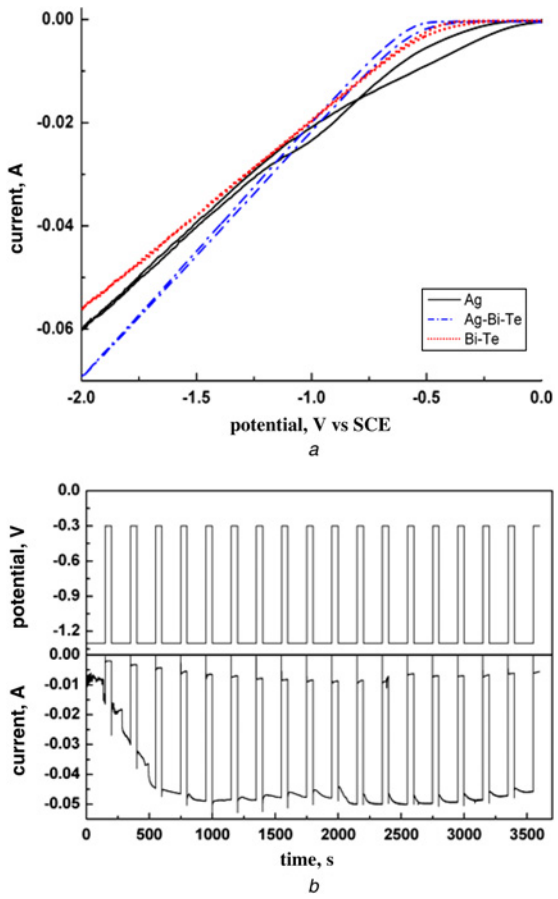

Figure 1 *Cyclic voltammograms of Ag–Bi–Te solution, Ag solution and Bi–Te solution (Fig. 1a), and Applied pulsed potential waveform and corresponding current response for deposition of Ag/Bi_2Te_3 SLNWs (Fig. 1b)*

The chemical composition and phase structure of the as-grown SLNWs with AAO templates were studied by XRD as shown in Fig. 2. The nine peaks marked with red colour in Fig. 2 can be easily indexed to (0 1 5), (1 0 10), (0 1 11), (0 0 15), (2 0 5), (0 0 18), (0 2 10), (1 1 15) and (2 1 10) planes of the Bi_2Te_3 rhombohedral lattice phase according to JCPDS Card Number 15-0863. At the same time, there are three main peaks marked with blue colour in Fig. 2, which indexed to (1 1 1), (2 2 0) and (3 1 1) planes of the Ag cubic lattice phase (JCPDS Card Number 04-0783). A careful examination indicates that there are some weak peaks in the XRD pattern at about 30° and 49°, which can be indexed to (110) and (13-1) planes of Te as marked with black colour. Thus, the XRD data indicates that the as-prepared SLNWs are mostly composed of the Bi_2Te_3 rhombohedral lattice phase and the Ag cubic lattice phase.

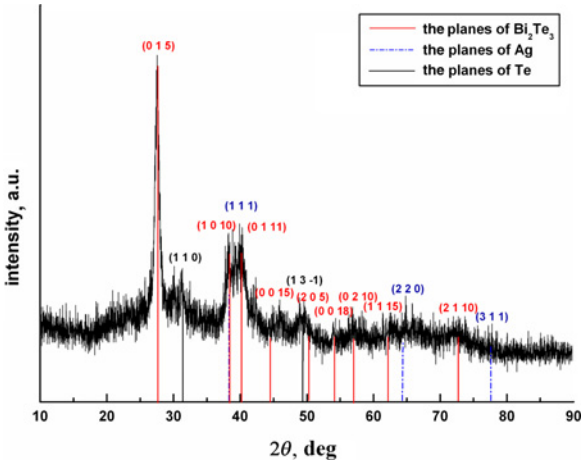

Figure 2 *XRD pattern of as-prepared SLNW arrays with AAO templates*

Fig. 3*a* shows the top view SEM image of the SLNW after the template was partially removed. The result indicates that the filling ratio is very high. Fig. 3*b* shows the oblique view SEM image of SLNW arrays after removing the templates, showing that large-scale nanowire arrays with a high-aspect ratio are obtained. The average diameter of the nanowires is about 70 nm. The segments alternately ordered can be easily distinguished in Fig. 3*b*.

To investigate the microstructure of the as-prepared SLNW clearly, the TEM image of the as-prepared SLNW arrays after removal of the AAO template is shown in Fig. 4*a*. The feature of dark segments alternated with bright segments can be easily distinguished because of the obvious heterogeneous contrast. The length of each segment is different, varying from 25 to 45 nm. A couple of neighbouring segments marked A and B were randomly selected. The length of segment A is about 35 nm, and segment B is about 27 nm. Fig. 4*b* gives the high-resolution transmission electron microscopy (HRTEM) image of two segments. The selected areas marked A and B by a square are corresponding to the lattice structure of A and B segments, respectively. The lattice spacing and growth direction in two selected areas are different, which indicates that the nanowire arrays of two segments were formed by two different compositions. For studying the compositions of two segments exactly, Figs. 4*c* and *d* are the enlarged images of selected areas marked A and B in Fig. 4*b*, respectively. The lattice

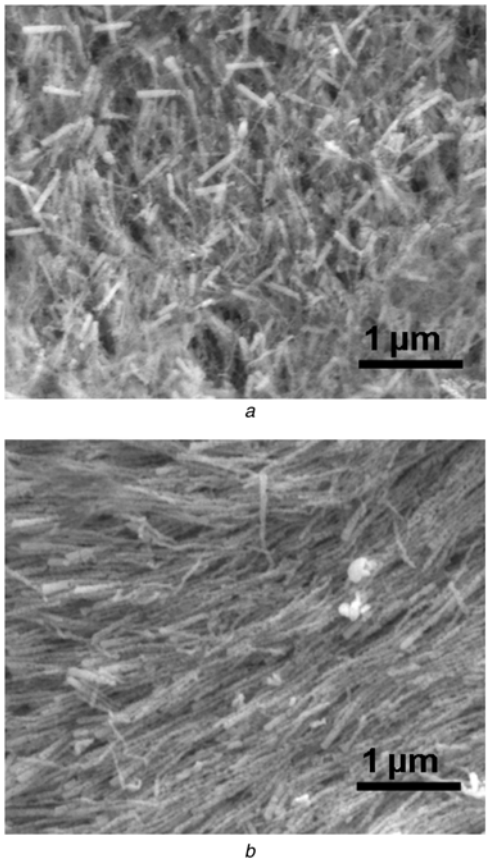

Figure 3 *SEM images of nanowire arrays*
a Top view
b Oblique view

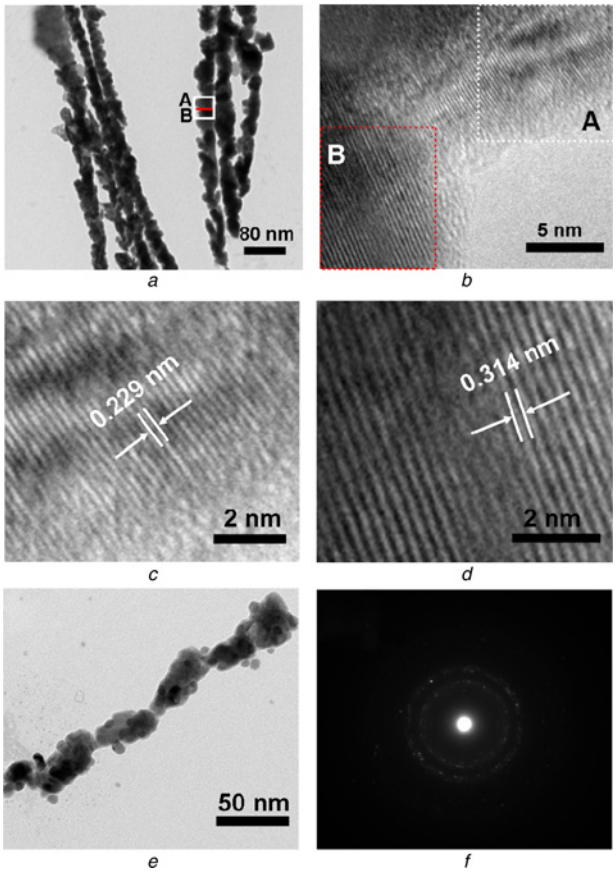

Figure 4 *TEM and HRTEM images, and selected area electron diffraction pattern of corresponding nanowire*
a TEM images of the as-prepared SLNW arrays
b HRTEM image of A and B segments
c Enlarged images of selected area marked A in Fig. 4b
d Enlarged images of selected area marked B in Fig. 4b
e Enlarged TEM image of Ag/Bi_2Te_3 SLNW
f Selected area electron diffraction pattern of corresponding nanowire

spacing of 0.229 nm in Fig. 4*c* corresponds to the lattice of (111) crystal plane of the Ag cubic lattice phase within the error. The lattice spacing in Fig. 4*d* is about 0.314 nm, which is consistent with the lattice space of (015) plane of the Bi_2Te_3 rhombohedral lattice phase in the error. These results show that the composition of segment A is Ag and segment B is Bi_2Te_3. Thus, the thermoelectric Ag/Bi_2Te_3 SLNW arrays were successfully prepared by pulse electrochemical deposition in this study. The above HRTEM investigations indicated that the as-prepared Ag/Bi_2Te_3 SLNWs were not crystallised, this can be further confirmed by the selected area electron diffraction pattern (taken from Fig. 4*e*), in which the ring pattern was observed as shown in Fig. 4*f*.

4. Conclusions: We have successfully fabricated Ag/Bi_2Te_3 SLNWs by a simple pulse electrodeposition technology at large quantity. The XRD result shows that the SLNWs are composed of the Bi_2Te_3 rhombohedral lattice phase and the Ag cubic lattice phase. Large-scale nanowire arrays with a high-aspect ratio can be observed in the SEM image, and two kinds of segments alternately ordered can be easily distinguished in the TEM image because of the obvious heterogeneous contrast. The composition of one segment is Ag, and the neighbouring segment is Bi_2Te_3.

5. Acknowledgments: This work was supported by the National Natural Science Foundation of China (NSFC, grant no. 11074312), the Fundamental Research Funds for the Central Universities (grant no. 1112KYQN35), the '985 project' (grant no. 98507-012009) and the '211 project' of the Ministry of Education of China, National Innovation and Training (grant no GCCX 2012110014), and the Under-graduate Research Training Programme of Minzu University of China (grant numbers URTP 2012110009, URTP 2012110010).

6 References

[1] Snyder G.J., Toberer E.S.: 'Complex thermoelectric materials', *Nat. Mater.*, 2008, **7**, pp. 105–114
[2] Sales B.C.: 'Smaller is cooler', *Science*, 2002, **295**, pp. 1248–1249
[3] Hochbaum A.I., Chen R.K., Delgado R.D., *ET AL.*: 'Enhanced thermoelectric performance of rough silicon nanowires', *Nature*, 2008, **451**, pp. 163–167
[4] Li X.H., Zhou B., Pu L., *ET AL.*: 'Electrodeposition of Bi_2Te_3 and Bi_2Te_3 derived alloy nanotube arrays', *Cryst. Growth Des.*, 2008, **8**, pp. 771–775
[5] Deng Y., Xiang Y., Song Y.Z.: 'Template-free synthesis and transport properties of Bi_2Te_3 ordered nanowire arrays via a physical vapor process', *Cryst. Growth. Des.*, 2009, **9**, pp. 3079–3082
[6] Xiao F., Yoo B.Y., Lee K.H., *ET AL.*: 'Synthesis of Bi_2Te_3 nanotubes by galvanic displacement', *J. Am. Chem. Soc.*, 2007, **129**, pp. 10068–10069
[7] Venkatasubramanian R., Siivola E., Colpitts T.: 'Thin-film thermoelectric devices with high room-temperature figures of merit', *Nature*, 2001, **413**, pp. 597–602
[8] Cui J.L., Xiu W.J., Mao L.D., *ET AL.*: 'Thermoelectric properties of Ag-doped n-type $(Bi_2Te_3)_{0.9}$–$(Bi_{2-x}Ag_xSe_3)_{0.1}$ ($x = 0$–0.4) alloys prepared by spark', *J. Solid State Chem.*, 2007, **180**, pp. 1158–1162
[9] Yang J.Y., Chen R.G., Fan X.A., *ET AL.*: 'Thermoelectric properties of silver-doped n-type Bi_2Te_3-based material prepared by mechanical alloying and subsequent hot pressing', *J. Alloys Compd.*, 2006, **407**, pp. 330–333
[10] Li D.P., Wang G.Z., Yang Q.H.: 'Synthesis and photoluminescence of $InGaO_3(ZnO)_m$ nanowires with perfect superlattice structure', *J. Phys. Chem. C*, 2009, **113**, pp. 21512–21525
[11] Wu Y.Y., Fan R., Yang P.D.: 'Block-by-block growth of single-crystalline Si/SiGe superlattice nanowires', *Nano Lett.*, 2002, **2**, pp. 83–86
[12] Wang W., Lu X.L., Zhang T., *ET AL.*: 'Bi_2Te_3/Te multiple heterostructure nanowire arrays formed by confined precipitation', *J. Am. Chem. Soc.*, 2007, **129**, pp. 6702–6703
[13] Choi J.R., Oh S.J., Ju H., *ET AL.*: 'Massive fabrication of free-standing one-dimensional Co/Pt nanostructures and modulation of ferromagnetism via a programmable barcode layer effect', *Nano Lett.*, 2005, **5**, pp. 2179–2183
[14] Xue F.H., Fei G.T., Wu B., *ET AL.*: 'Direct electrodeposition of highly dense Bi/Sb superlattice nanowire arrays', *J. Am. Chem. Soc.*, 2005, **127**, pp. 15348–15349
[15] Wang W., Zhang G.Q., Li X.G.: 'Manipulating growth of thermoelectric Bi_2Te_3/Sb multilayered nanowire arrays', *J. Phys. Chem. C*, 2008, **112**, pp. 15190–15194
[16] Wang W., Zhang G.Q., Li X.G.: 'Kinetic versus thermodynamic control over growth process of electrodeposited Bi/BiSb superlattice nanowires', *Nano Lett.*, 2008, **8**, pp. 1286–1290
[17] Yoo B.Y., Xiao F., Bozhilov K.N., *ET AL.*: 'Electrodeposition of thermoelectric superlattice nanowires', *Adv. Mater.*, 2007, **19**, pp. 296–299

doi: 10.1049/mnl.2012.0850